CHAPTER IV
RESULTS AND DISCUSSION

4.1 Adsorbent Modification and Characterizations

The objective of this part was to carry out a comprehensive investigation in the preparation of modified zeolites (NiX, NiY, $Cu^{(I)}Y$) by using two different techniques, LPIE and STIE, to load metal. The effect of temperature and the amount of metal ions on metal loading using LPIE technique were discussed. Moreover, the comparison between two techniques was also presented.

4.1.1 Ni-exchanged zeolites prepared by liquid phase ion-exchanged technique in a batch reactor

4.1.1.1 Effect of temperature on metal loading

The amount of Ni-loading on NaX and NaY zeolites was measured by using an Atomic Absorption Spectrometer – AAS (Varian, SpectrAA 300 model). In the experiments, the concentration of metal solution and solution/adsorbent ratio were fixed at 0.01 mol/l and 200:1, respectively. The temperature was varied in the range of 30°C to 150°C. The results are shown in Figure 4.1.

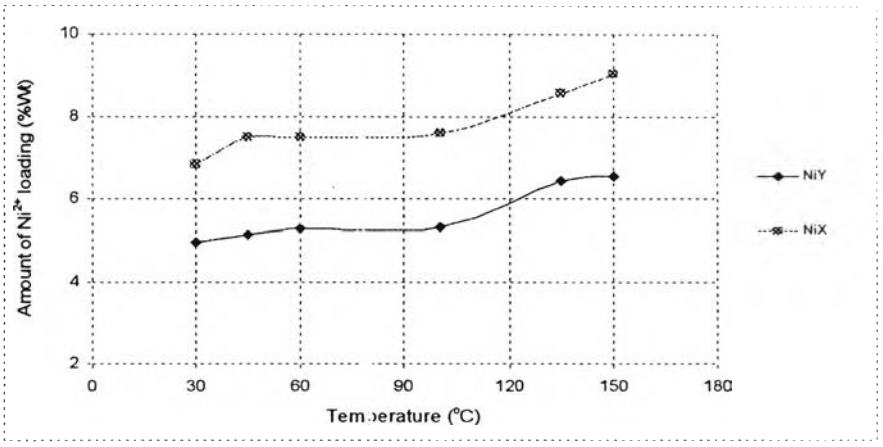

Figure 4.1 Effect of temperature on metal loading.

It has been reported that the degree of exchange by LPIE technique is limited not only by the thermodynamic equilibrium but also by the steric constraints due to the formation of solvatation of the exchangeable cations in the aqueous solution. One of several effective ways to overcome this undesirable phenomenon is increasing temperature during the ion-exchange process. Figure 4.1 shows that the amount of metal loading on zeolite increased with raising temperature due to faster diffusion rates of metal ions into the zeolite pores. Beside, the increased in temperature supplied energy of dehydration and caused better vibration of the aluminosilicate framework. However, using high temperature during ion-exchanging undesirably results in a collapse of zeolite's framework; markedly in the case of NaX zeolite, which contains a high concentration of aluminum atoms per cell, it displayed comparatively low thermal stabilities.

The BET surface area of NaX and NaY zeolites before and after exchanged at different temperatures were determined by using Sorptomatic SAA (Themo Finnigan), which are listed below in Table 4.1.

Table 4.1 Surface area of sorbents

Adsorbents	BET surface area (m^2/g)
NaX zeolite	639
NiX zeolite, 45°C	480
NiX zeolite, 60°C	284
NaY zeolite	639
NiY zeolite, 135°C	452
NiY zeolite, 150°C	127

According to Table 4.1, the surface area of NaX was significantly decreased when the exchange process temperature was higher than 60°C, whereas the change in NaY's surface area markedly decreased when the temperature was above

135°C. Hence the optimum temperatures for achieving sufficient amount of metal loading on NaX and NaY were chosen to be 45°C and 135°C, respectively.

4.1.1.2 Effect of the amount of metal ions on metal loading

In the experiments, the concentration of metal solution was fixed at 0.01 mol/l, and the exchange process temperature was set at 45°C for NaX zeolite and 135°C for NaY zeolite. Solution to adsorbent ratio was varied from 50:1 to 200:1. The results are summarized in Figure 4.2.

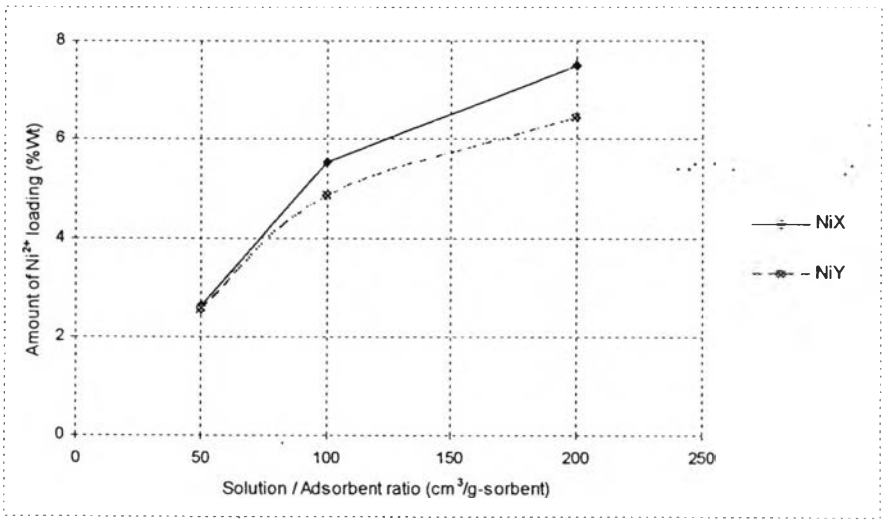

Figure 4.2 Effect of the amount of metal ions on metal loading.

As seen in Figure 4.2, the amount of Ni^{2+} loading on NaX and NaY zeolites were proportional to the amount of solution to adsorbent ratio in exchanging process. Furthermore, as compared with NaY zeolite, NaX zeolite showed higher ion-exchange capacity. The explanation will be discussed in next part, ion-exchange isotherm.

4.1.1.3 Ion-exchange isotherm

The selectivity of an ion-exchange process was constructed by the ion-exchange isotherm which describes the situation after equilibrium. In this experiment, the equivalent fraction of the entering cation Ni^{2+} in solution $E_{Ni(S)}$ was plotted against the equivalent fraction for the same cation in the zeolite phase E_{Ni}. The temperature was fixed at 45°C for NaX zeolite and at 135°C for NaY. The results are shown in Figure 4.3.

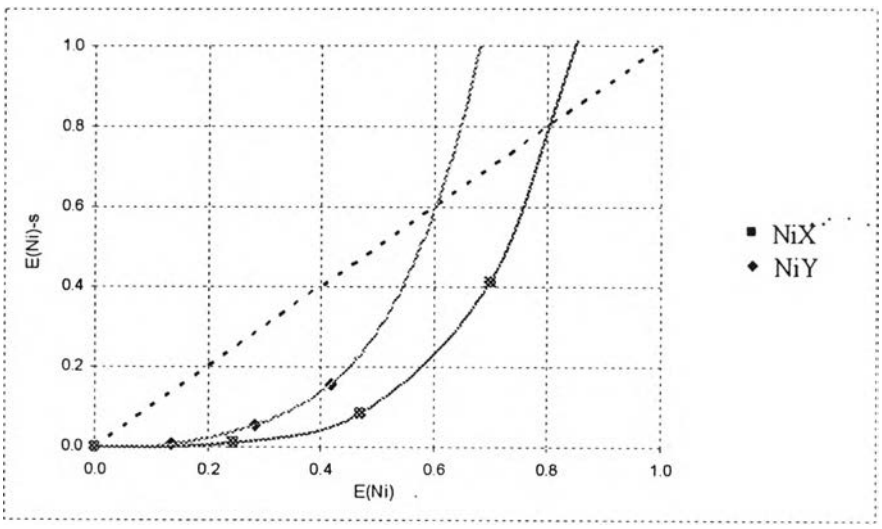

Figure 4.3 Ion-exchange isotherm for the NiX (at 45°C) and the NiY (at 135°C).

From Figure 4.3, both ion-exchange isotherm of NiX and NiY lie under the selectivity line which is drawn through points (0, 0) and (1, 1). It means that both NaX and NaY zeolites are exchangeable with Ni^{2+} ion. In addition, the metal isotherms also showed that a complete exchange (100%) was not achieved in both cases. Apparently 85% of the total Na^+ in the NaX zeolite and 68% of the total Na^+ in the NaY could be replaced by Ni^{2+}. The reason for this incomplete substitution lies in the structure of faujasites-type zeolites, in which the Na^+ ions are located in the sodalite

cages. Thus it is very difficult for the larger cations (Ni^{2+}) to diffuse through the diameter window between the super cage and the sodalite cage.

In comparison with NaY, NaX zeolite registered a higher ion-exchange capacity. The difference in the ion-exchange capacity between zeolite X and Y can be explained in terms of the location of the cations (Na^{+}) that balance the negative charges on the aluminosilicate framework. The number of aluminum ions per unit cell varies from 96 to 77 (Si/Al = 1 to 1.5) for type X, and from 76 to 48 (Si/Al = 1.5 to 3) for type Y zeolites.

4.1.1.4 X-ray Diffraction Spectroscopy (XRD)

X-ray Diffraction Spectroscopy was employed to characterize the crystallinities and phases of zeolite before and after ion exchange by LPIE technique as seen in Figure 4.4 (a, b).

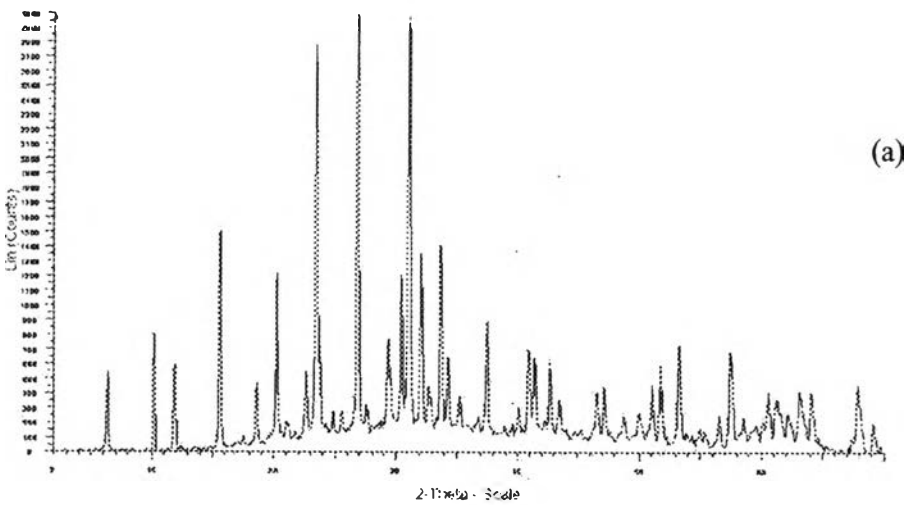

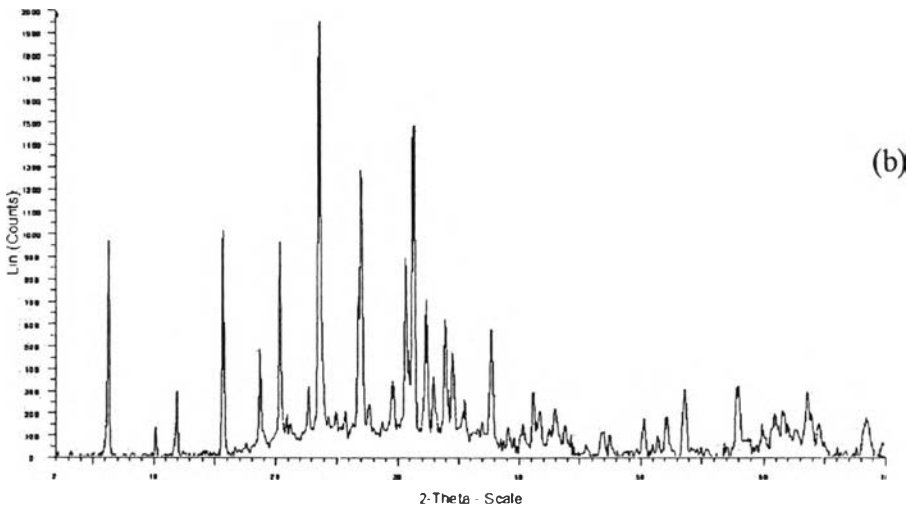

Figure 4.4 Comparison of XRD pattern of (a) NaX, and (b) NiX (7.48%wt Ni) at 45°C.

In Figure 4.4 (a, b), the XRD powder pattern of the prepared NiX zeolite was almost the same as the original structure of NaX zeolite. It indicates that the structure of the zeolite remained intact after treatment procedures.

4.1.2 Ni-exchanged zeolites prepared by solid state ion-exchanged technique

Besides the conventional liquid phase ion-exchanged technique (LPIE), solid state ion-exchange (SSIE) plays an increasing role in the preparation of modified zeolites, where a high degree of exchange can be achieved (as high as 100% exchange) in only one step in addition to the fact that the limitations found from LPIE method can be overcome. Some advantages of SSIE are listed here (Hernandez *et al*, 2004):

- Avoiding the use of large volumes of salt solution
- Avoiding the problem of discarding waste salts solution
- Allowing the metal cations (which are small) to be introduced through narrow windows or channels that would impede or prevent the ion exchange of solvated from aqueous solution

The X-ray Diffraction Spectrum of the NaY zeolite before and after ion exchange by SSIE technique is shown in the Figure 4.5 (a, b).

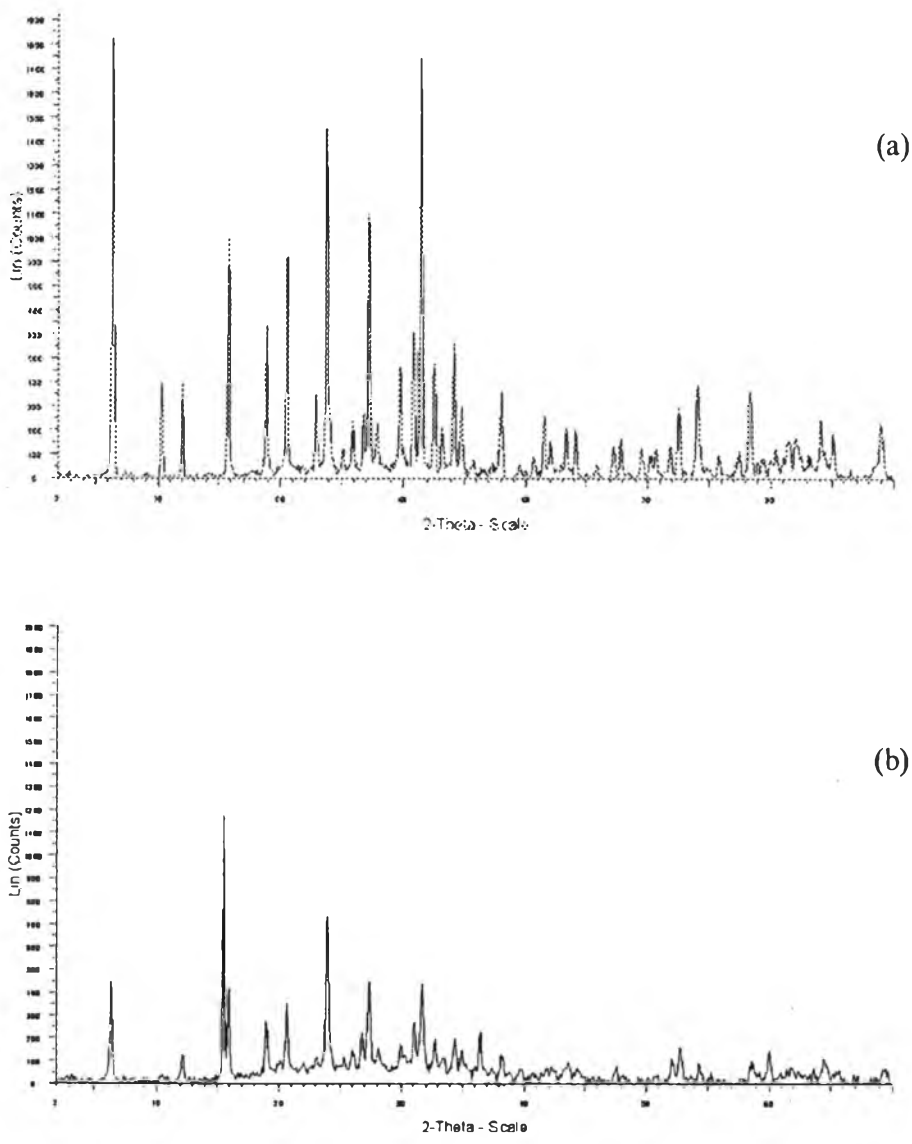

Figure 4.5 Comparison of XRD pattern of (a) NaY, and (b) NiY-SSIE method (9.17%wt Ni).

The XRD patterns of the NiY samples indicated that these samples retain the original zeolite structure, although the intensities of the peaks weaken. This excludes the occurrence of partial crystal collapse due to solid-state exchange treatment.

The amount of Ni loading by liquid-phase ion-exchanged method was limited to 6.4%wt Ni loading - corresponding to 68% ion-exchanged degree whereas the solid-state ion-exchanged could incorporate higher Ni content in the sorbent (9.2%wt Ni) and also obtained 100% ion-exchanged degree. The comparison regarding composition and surface area of samples prepared by these two methods are illustrated in the Table 4.2. Consequently, this study focused on using solid-state ion exchange method for NaY zeolite because NaX zeolite had shown to have low thermal stabilities and thus was not chosen to study here.

Table 4.2 Metal ion-exchange and surface area of samples between two methods

Preparation	**Liquid phase ion-**	**Solid state ion-exchanged method**	
Ni ion content (mg/g-zeolite)	6.42	Analysis no.1	9.0
		Analysis no.2	9.2
Ion exchange degree (%)	68	Analysis no.1	99.1
		Analysis no.2	100.1
BET area (m^2/g)	512	Analysis no.1	350.6
		Analysis no.2	324.4

4.1.3 Characterization of the adsorbents

By using Mercury porosimetry and Nitrogen adsorption/desorption methods, properties of the pore structure and also specific surface area of adsorbents used in this study are presented in Tables 4.3 and 4.4.

Table 4.3 Properties of adsorbents by using the Nitrogen adsorption / desorption methods

Properties	NaX	NiX (7.48%wt Ni)
B.E.T. Surface Area (m^2/g)	619	512
Vμ (t-plot) (cm^3/g)	0.235	0.086
Vμ (Dubinin) (cm^3/g)	0.249	0.139
Vμ+Vm (cm^3/g)	0.375	0.310
Vm (cm^3/g)	0.140	0.224

Properties	NaY	NiY	CuY
B.E.T. Surface Area (m^2/g)	639	591	560
Vμ (t-plot) (cm^3/g)	0.253	0.227	0.215
Vμ (Dubinin) (cm^3/g)	0.271	0.246	0.239
Vμ+Vm (cm^3/g)	0.452	0.382	0.361
Vm (cm^3/g)	0.199	0.155	0.146

Table 4.4 Properties of adsorbents by using the Mercury porosimetry

Properties	NaX	NiX (7.48%wt Ni)
Particle Density (g/cm^3)	0.983	1.044
Structural Density (g/cm^3)	1.645	1.911
Vm (cm^3/g)	0.078	0.127
VM (cm^3/g)	0.258	0.240
Vm+VM (cm^3/g)	0.336	0.367

Properties	NaY	NiY	CuY
Particle Density (g/cm^3)	0.982	0.999	0.649
Structural Density (g/cm^3)	1.625	1.682	1.672
Vm (cm^3/g)	0.051	0.051	0.089
VM (cm^3/g)	0.282	0.308	0.314
Vm+VM (cm^3/g)	0.333	0.360	0.404

4.2 Static Adsorption of Sulfur Compounds in Simulated Fuels

In this part, the Ni-exchanged X-type zeolites, including the original zeolite, were evaluated for their efficiency in removing model sulfur compounds, 3-MT and BT in both binary and ternary systems of isooctane and benzene used as simulated transportation fuel. The ratio of fuel to adsorbent was fixed at 85:1. Besides, the experiments were carried out on a batch reactor and operated at ambient conditions.

4.2.1 Static adsorption in a binary system

4.2.1.1 Static adsorption of sulfur compounds in isooctane

The potential of a set of NiX-zeolites with different amount of metal loading was investigated for the sulfur adsorption capacity in isooctane. The concentration of initial sulfur compounds in isooctane was varied from 500 ppmw to 2500 ppmw. Subsequently, the adsorption isotherms of 3MT and BT in isooctane were constructed by plotting the sulfur adsorbed amount against the equilibrium concentration. The results showing the impact of different amount of Ni^{2+} loading on NaX zeolite to adsorption isotherms are presented in Figure 4.6 and Figure 4.7.

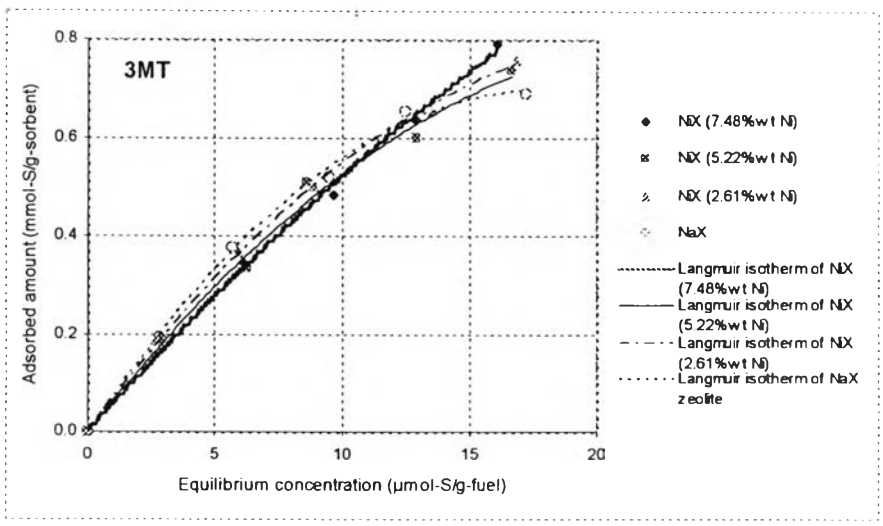

(a)

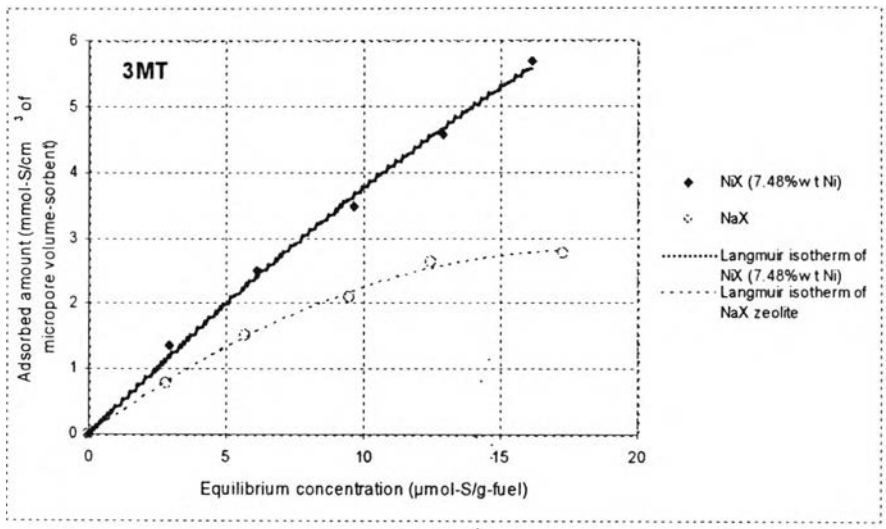

(b)

Figure 4.6 Adsorption isotherms of 3-methylthiophene in isooctane by NiX zeolite with different amount of Ni^{2+} loading. a) 3-MT adsorbed per game of adsorbent, b) 3-MT adsorbed per cm^3 of micropore volume of adsorbent.

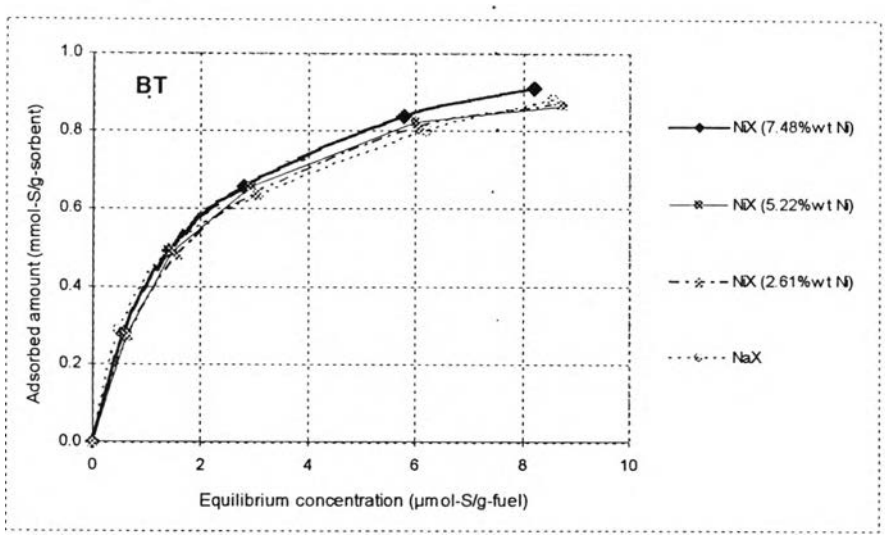

(a)

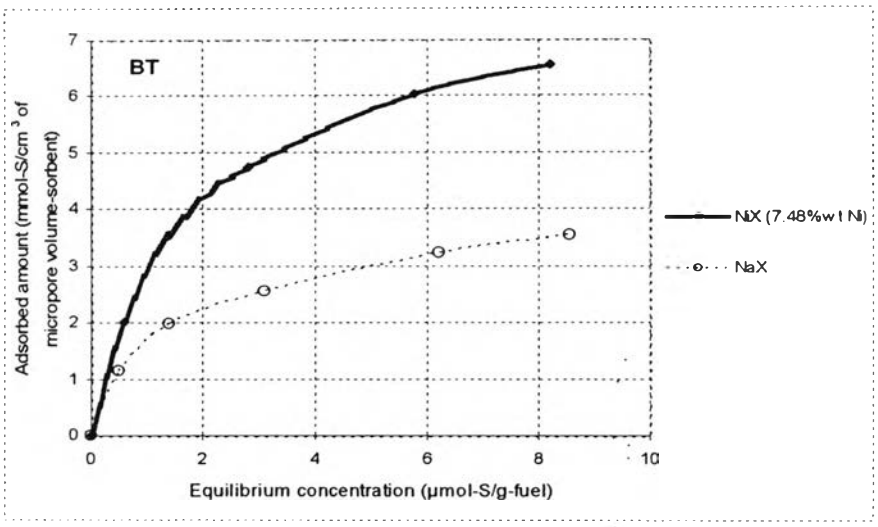

(b)

Figure 4.7 Adsorption isotherms of benzothiophene in isooctane by NiX zeolite with different amount of Ni^{2+} loading. a) BT adsorbed per game of adsorbent, b) BT adsorbed per cm^3 of micropore volume of adsorbent.

The experimental data of the adsorption of 3-MT and BT in isooctane on NiX zeolites were well-fitted with Langmuir isotherm, which could be explained by the Langmuir monolayer adsorption model. The Langmuir equation is obtained:

$$Q_s = \frac{Q_{max} b C_s}{1 + b C_s}$$

Or the Langmuir isotherm is presented in the linear form:

$$\frac{C_S}{Q_S} = \frac{1}{Q_{max} b} + \frac{C_S}{Q_{max}}$$

Where: Q_s and Q_{max} are the sulfur uptake (mmol-S/g-sorbent) and the maximum adsorption capacity (mmol-S/g-sorbent), respectively; C_S is the

equilibrium sulfur concentration (mmol-S/g-fuel); b is a constant of sulfur adsorption (g-fuel/mmol). Moreover, an estimation of the Henry constants can be applied from these parameters, since the Langmuir equation can be simplified into the linear relation $Q_s/C_S = Q_{max}.b$ in the low concentration range. The Langmuir parameters including the corresponding values for $K_H = Q_{max}.b$ are presented in Table 4.5 for 3-MT and in Table 4.6 for BT.

Table 4.5 Langmuir parameters of the adsorption of 3-MT in isooctane by NiX zeolites

Adsorbent	Q_{max} (mmol-S/g-sorbent)	b (g-fuel/μmol-S)	K_H (g-fuel/g-sorbent)
NaX	1.6998	0.0468	79.55
NiX (2.61%wt Ni)	1.6866	0.0474	79.94
NiX (5.22%wt Ni)	1.7467	0.0419	73.19
NiX (7.48%wt Ni)	1.7768	0.0416	73.91

Table 4.6 Langmuir parameters of the adsorption of BT in isooctane by NiX zeolites

Adsorbent	Q_{max} (mmol-S/g-sorbent)	b (g-fuel/μmol-S)	K_H (g-fuel/g-sorbent)
NaX	0.9088	0.9334	848.27
NiX (2.61%wt Ni)	1.0705	0.5070	542.74
NiX (5.22%wt Ni)	1.0641	0.5623	598.34
NiX (7.48%wt Ni)	1.0746	0.6044	649.49

From the experiment data, we noticed that the Langmuir isotherm for 3-MT adsorption was similar to BT adsorption. It can be observed that for both 3-MT and BT, the sulfur adsorption were not much different when increasing the amount of Ni^{2+} loading on the zeolite. The result indicated that the amount of sulfur compounds adsorbed was independent of the amount of Ni^{2+} loading. This may be caused by a small

portion of metal ions not located in exposed adsorption sites. Another reason may be that the structure of zeolite was re-crystallized during ion exchange treatment. Furthermore, as seen in Table 4.3, the microspore volume of NiX (0.139 cm^3/g) was significantly less than that of NaX (0.249cm^3/g). It means the original zeolite contained much more α-cages than the other. Hence, with the relatively equivalent amount of sulfur compounds adsorbed per g zeolite (1.6998 mmol 3-MT/g-sorbent, 0.9088 mmol BT/g-sorbent for NaX; 1.7768 mmol 3-MT/g-sorbent, 1.0746 mmol BT/g-sorbent for NiX), Ni-exchanged zeolite exhibited higher sulfur adsorption capacity, as compared with NaX zeolite (as seen in Figures 4.6b and 4.7b). This clearly illustrated the forming of π-complexation between sulfur compounds and Ni^{2+}, since Na^+ ions could not create π-complexation bonds. The small difference regarding the maximum capacity between adsorption on the metal ion-exchanged zeolites and original zeolite was due to the remaining sodium ions in the zeolite structure after exchanging by LPIE method. Moreover, the effect of types of sulfur compounds to adsorption in NiX zeolites is displayed in Figure 4.8.

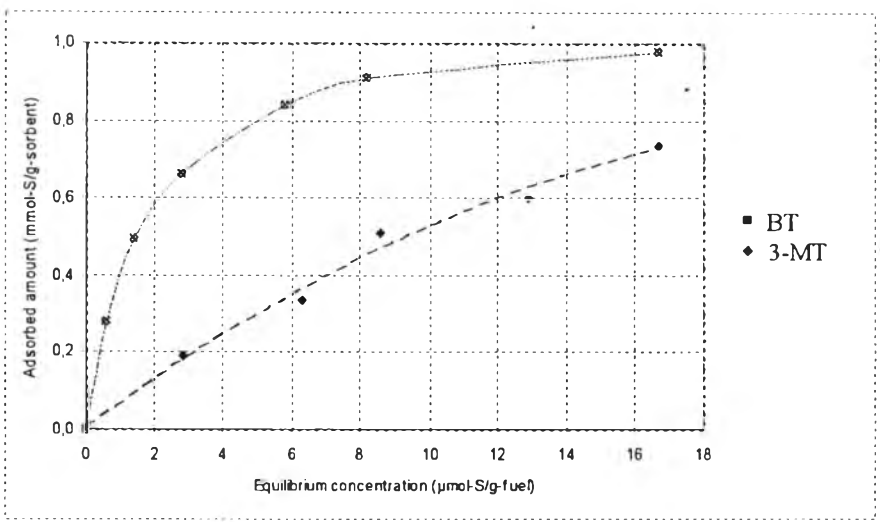

Figure 4.8 Adsorption isotherms with different sulfur compounds on NiX zeolite (7.48%wt Ni) in isooctane as the model fuel.

According to the Langmuir parameters, the saturation capacity (Q_{max}) for 3-MT is 1.6 times as much as that for BT but at much higher equilibrium sulfur concentration. It may be due to the fact that BT molecules have larger size as compared to 3-MT. Interestingly, BT adsorption isotherms appeared to be much steeper than those of 3-MT, especially in low concentration range. This reflects a higher strength of adsorption, corresponding well with a high affinity constant (b) in case of BT. The higher b value is likely due to the fact that BT represented two aromatics rings containing high electron density, which can strongly interact with transition Ni^{2+} ions via π-complexation forming. In other words, BT had higher affinity with metal ion-exchanged zeolite than 3-MT.

4.2.1.2 Adsorption of sulfur compounds in benzene

As transportation fuels also contain aromatics, such as benzene, toluene, xylene, as high as 30% of the total, it is necessary to evaluate the effect of aromatics content on the desulfurization process. Thus, benzene was used as transportation fuel model instead of isooctane. The results showing the influence of different amount of Ni^{2+} loading on NaX zeolite to adsorption isotherms are shown in Figure 4.9 and Figure 4.10.

When benzene was used as model fuel, the isotherms look quite similar to those observed in isooctane case but both adsorption capacities and affinity constants were much lower than those of the system of isooctaneas seen in Table 4.7 and 4.8 for 3-MT adsorption and BT adsorption, respectively.

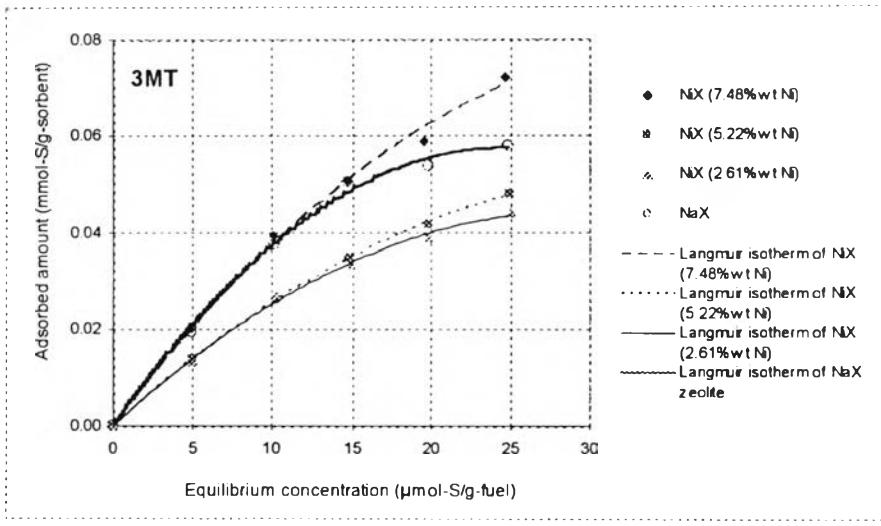

Figure 4.9 Adsorption isotherms of 3-methylthiophene in benzene by NiX zeolites with different amount of Ni^{2+} loading.

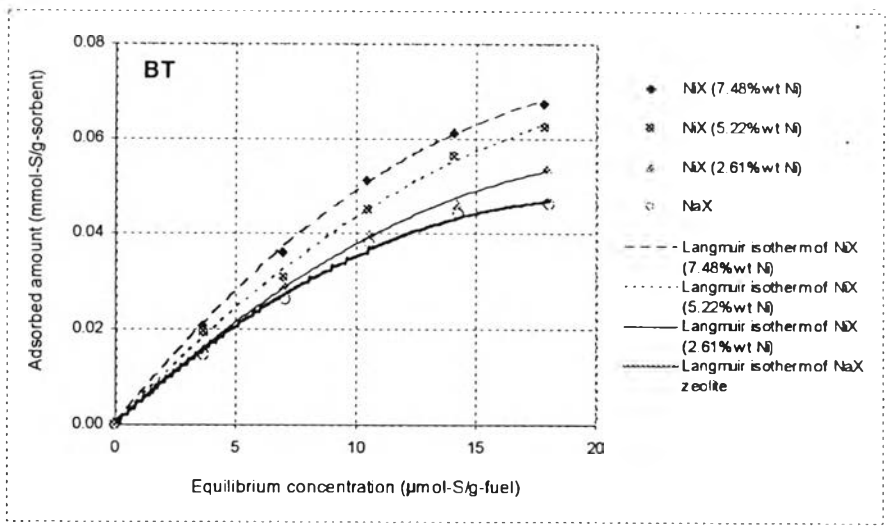

Figure 4.10 Adsorption isotherms of benzothiophene in benzene by NiX zeolites with different amount of Ni^{2+} loading.

Table 4.7 Langmuir parameters of the adsorption of 3-MT in benzene by NiX zeolite

Adsorbent	Q_{max} (mmol-S/g-sorbent)	b (g-fuel/μmol-S)	K_H (g-fuel/g-sorbent)
NaX	0.1498	0.0304	4.55
NiX (2.61%wt Ni)	0.1209	0.0253	3.06
NiX (5.22%wt Ni)	0.1266	0.0250	3.16
NiX (7.48%wt Ni)	0.1936	0.0240	4.65

Table 4.8 Langmuir parameters of the adsorption of BT in benzene by NiX zeolite

Adsorbent	Q_{max} (mmol-S/g-sorbent)	b (g-fuel/μmol-S)	K_H (g-fuel/g-sorbent)
NaX	0.1407	0.0316	4.45
NiX (2.61%wt Ni)	0.1448	0.0346	5.01
NiX (5.22%wt Ni)	0.1471	0.0408	6.00
NiX (7.48%wt Ni)	0.1837	0.0351	6.45

The adsorption equilibrium constant dropped approximately to half for both types of sulfur compounds while the saturation capacity decreased by 5.8 times for BT adsorption and by 9.8 times for 3-MT adsorption. The results revealed that the removal rate and the overall sulfur uptake capacity of the sorbents were significantly reduced when benzene was present, which can be attributed to the competitive π-complexation forming with the adsorbent between aromatic (benzene) and sulfur compounds.

4.2.2 Static adsorption of sulfur compounds in ternary system

4.2.2.1 Effect of aromatic content on sulfur compounds adsorption

As discussed above, in view of large aromatic content (benzene used as the model fuel), we believed that there was a competition between aromatic (benzene) and sulfur compounds (3-MT and BT) getting adsorbed on zeolites. In order to obtain a clearer picture on the effect of aromatics in the desulfurization of transportation fuels, this experiment focused on a small range of benzene concentration (0 to 15% by weight) in a solution of isooctane and 2000 ppmw sulfur content. NiX zeolite with the highest metal loading (7.48%wt Ni) and original NaX zeolite were chosen for testing. The results are shown in Figure 4.11 and Figure 4.12.

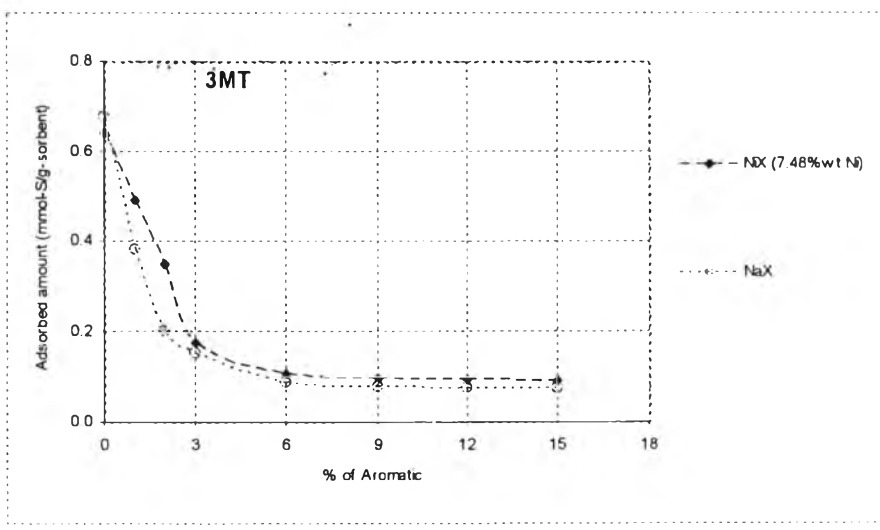

Figure 4.11 Effect of aromatics content on 3-MT adsorption on NiX (7.48%wt Ni) and NaX.

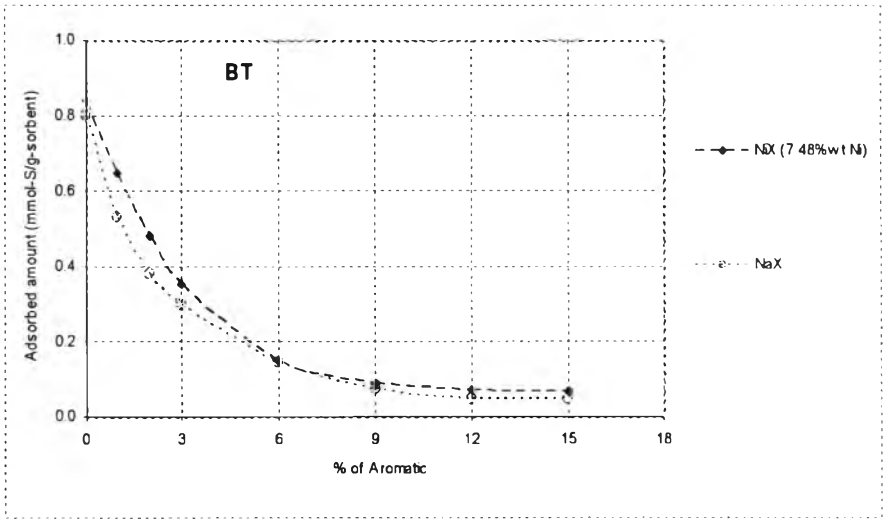

Figure 4.12 Effect of aromatic content on BT adsorption on NiX (7.48%wt Ni) and NaX.

From Figure 4.11 and Figure 4.12, the results illustrated a dramatic reduction in the sulfur uptake with increasing aromatics concentration. The drastic drop on adsorption capacity was found to be approximately 73% for 3MT and 58% for BT when benzene concentration reached to 3% and 6%, respectively. From that point on, the change was not significant. The influence of aromatic content could be explained from the fact that benzene can compete with 3-MT and BT for entering zeolite pores and adsorbing on the active sites of the zeolite. Even with benzene presented as co-adsorbate, the exchanged zeolite still exhibited a higher affinity towards sulfur compounds than the original one. In other words, the interaction between sulfur compounds and the exchanged zeolite seemed to be ruled by π-complexation. Therefore, it could be safely concluded that the π-complexation sorbent is more favorable in desulfurization application.

4.2.2.2 Competitive adsorption between sulfur compounds and benzene on zeolite

Results for sulfur compounds and benzene adsorption on NiX (7.48%wt Ni) and original NaX zeolites from different concentrations of benzene (0 to 15% by weight) in solution of isooctane and 2000 ppmw sulfur content are presented in Figures 4.13 and 4.14, giving more insights about the impact of aromatics on sulfur removal process.

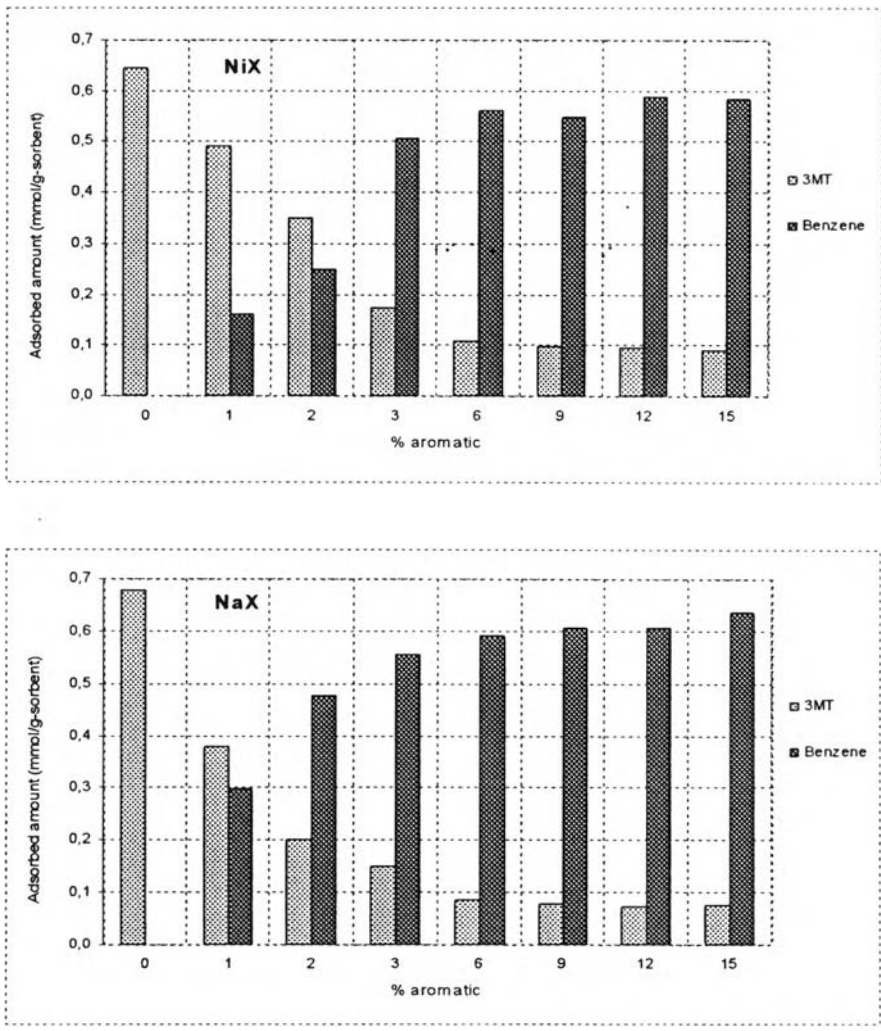

Figure 4.13 3-MT and benzene adsorption on (a) NiX (7.48%wt Ni), and (b) NaX zeolites from different concentrations of benzene.

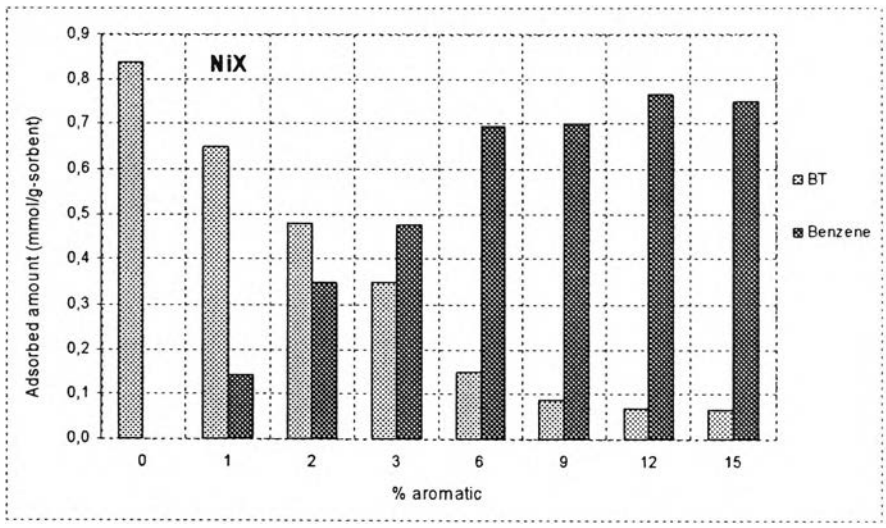

(a)

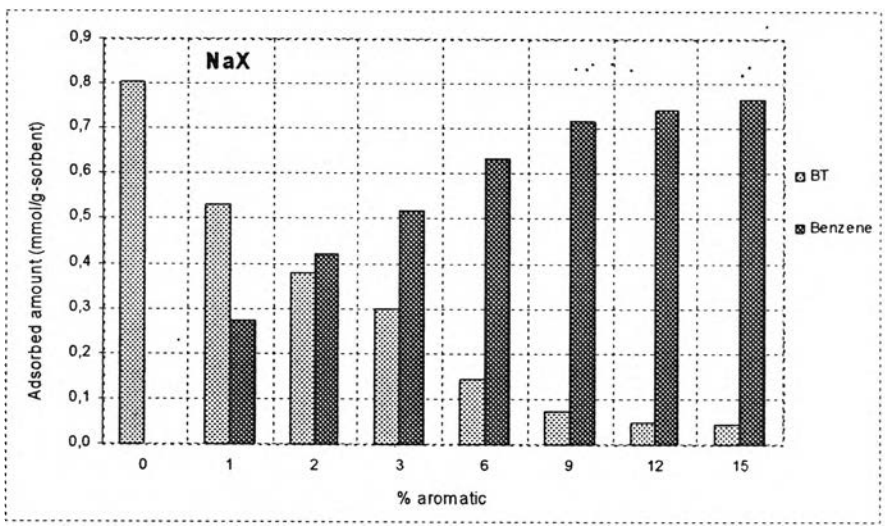

(b)

Figure 4.14 BT and benzene adsorption on (a) NiX (7.48%wt Ni), and (b) NaX zeolites from different concentrations of benzene.

In addition, Table 4.9 and 4.10 contain selectivity factors for sulfur compounds and benzene, helping to estimate how the sulfur compounds are favored over benzene in mixture solution, which were given in terms of number of moles of sulfur compounds and benzene adsorbed on zeolites.

Table 4.9 Selectivity factors of 3-MT over benzene in ternary system using NiX (7.48%wt Ni) and NaX zeolites.

Zeolite	Aromatic content (%)	Absorbed 3-MT (mmol/g-sorbent)	Adsorbed Benzene (mmol/g-sorbent)	Selectivity ($S_{3MT/Benzene}$)
NiX (7.48%wt Ni)	1%	0.492	0.161	3.063
	2%	0.356	0.254	1.400
	3%	0.173	0.506	0.342
	6%	0.108	0.561	0.192
	9%	0.098	0.549	0.179
	12%	0.095	0.589	0.161
	15%	0.091	0.585	0.155
NaX	1%	0.389	0.298	1.277
	2%	0.230	0.478	0.419
	3%	0.150	0.556	0.270
	6%	0.087	0.594	0.146
	9%	0.078	0.607	0.128
	12%	0.074	0.607	0.122
	15%	0.075	0.635	0.118

Table 4.10 Selectivity factors of BT over benzene in ternary system using NiX (7.48%wt Ni) and NaX zeolites.

Zeolite	Aromatic content (%)	Absorbed BT (mmol/g-sorbent)	Adsorbed Benzene (mmol/g-sorbent)	Selectivity ($S_{3MT/Benzene}$)
NiX (7.48%wt Ni)	1%	0.657	0.145	4.482
	2%	0.482	0.350	1.371
	3%	0.350	0.475	0.737
	6%	0.150	0.695	0.216
	9%	0.089	0.702	0.127
	12%	0.070	0.768	0.091
	15%	0.065	0.750	0.087
NaX	1%	0.538	0.272	1.948
	2%	0.387	0.422	0.900
	3%	0.298	0.518	0.577
	6%	0.144	0.634	0.227
	9%	0.075	0.718	0.104
	12%	0.048	0.744	0.064
	15%	0.046	0.766	0.060

As seen from Table 4.9 and Table 4.10, in case of low aromatic content (1%), the selectivity factors of 3-MT and BT over benzene were 3.06 and 4.48, respectively, for π-complexation sorbent (NiX zeolite); whereas for original zeolite (NaX), the selectivity factor decreased to 1.28 for 3-MT and 1.95 for BT. The results, again, confirmed the beneficial effect of exchanged zeolite on the adsorption selectivity of sulfur compounds in the presence of benzene. Moreover, those high values of selectivity factors at 1-2% benzene concentration also implied that sulfur compounds have higher strengths of π-complexation bonds than benzene. However, when increasing the aromatic content (over 3% wt), the experimental data showed a significant decrease of selectivity factors, effectively shifting the balance to benzene. These less-than-one values indicated that zeolites are more subject to be occupied by benzene than by sulfur compounds at this high level of benzene concentration. It could be explained that at these concentrations, despite sulfur compound's high strength of π-complexation bonds, the surface of zeolite had been completely saturated by benzene molecules, leaving very few active sites available for sulfur compounds to be bound.

It is also noted that at these high concentrations of benzene in our ternary system (up to 12% wt), the selectivity factors did not vary considerably. The results suggested a limited adsorption mechanism for sulfur compounds and benzene on zeolite. Not all active adsorption sites, which were able to bound by sulfur compounds, were suitable for benzene adsorption.

4.2.3 Effect of exchanged techniques in static adsorption

To study the effect of exchanged techniques in adsorption of sulfur compounds, the Langmuir isotherms of various zeolite adsorbents prepared by two different techniques, liquid-phase ion exchange (LPIE) and solid-state ion exchange (SSIE), were plotted together. The results are presented in Figure 4.15 (a, b) and Figure 4.16 (a, b) corresponding with the Langmuir parameters shown in Tables 4.11 and 4.12 for isooctane and benzene as environment fuels, respectively.

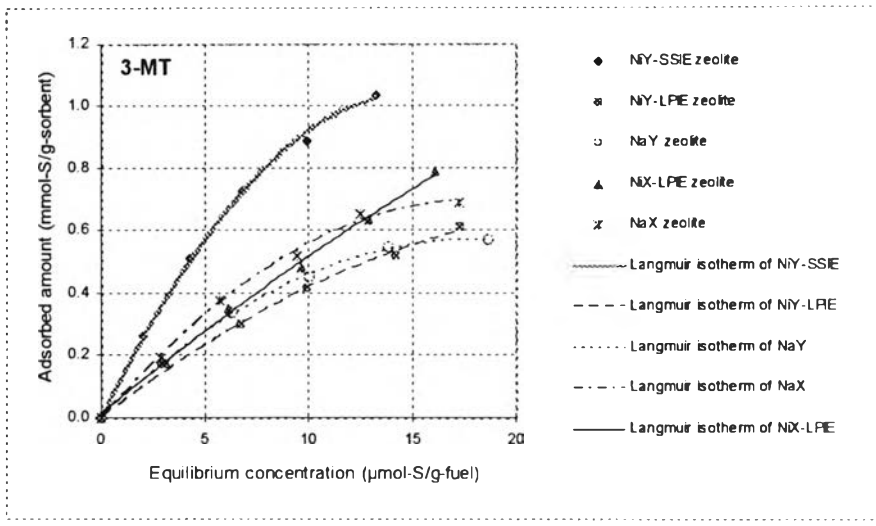

(a)

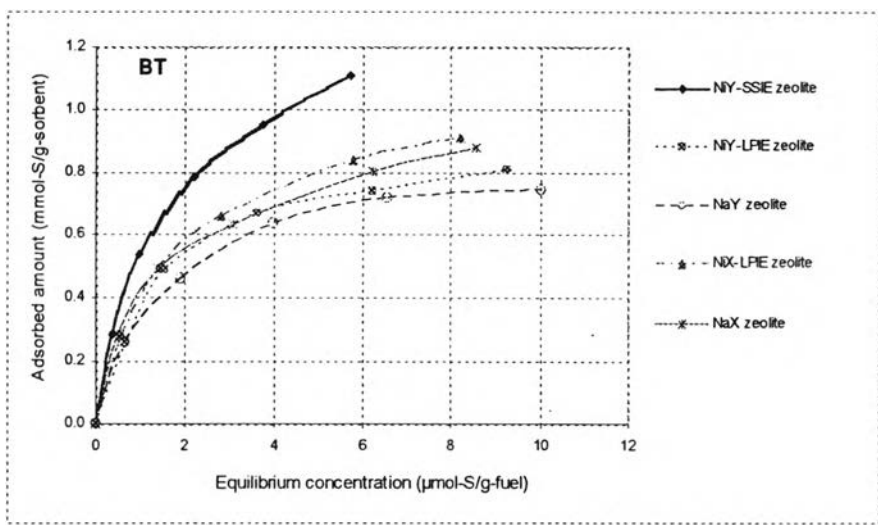

(b)

Figure 4.15 Adsorption isotherms of (a) 3-MT, and (b) BT in isooctane solution by various zeolite adsorbents.

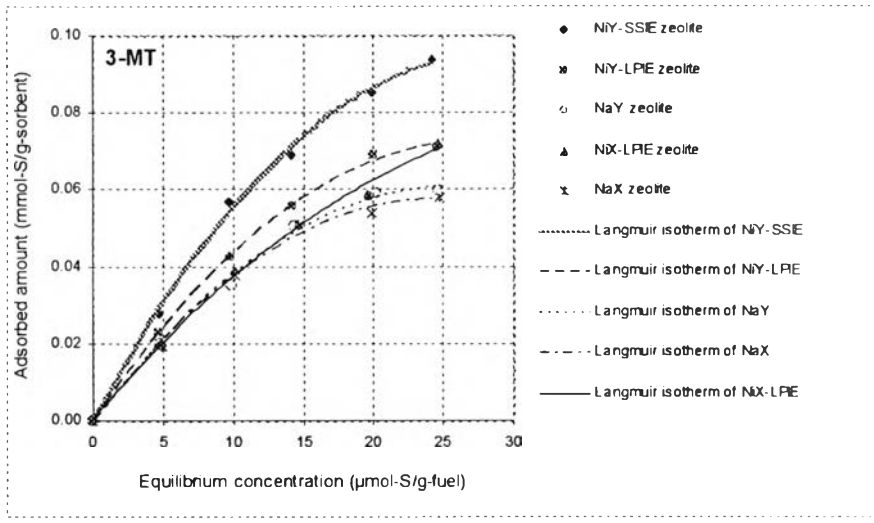

(a)

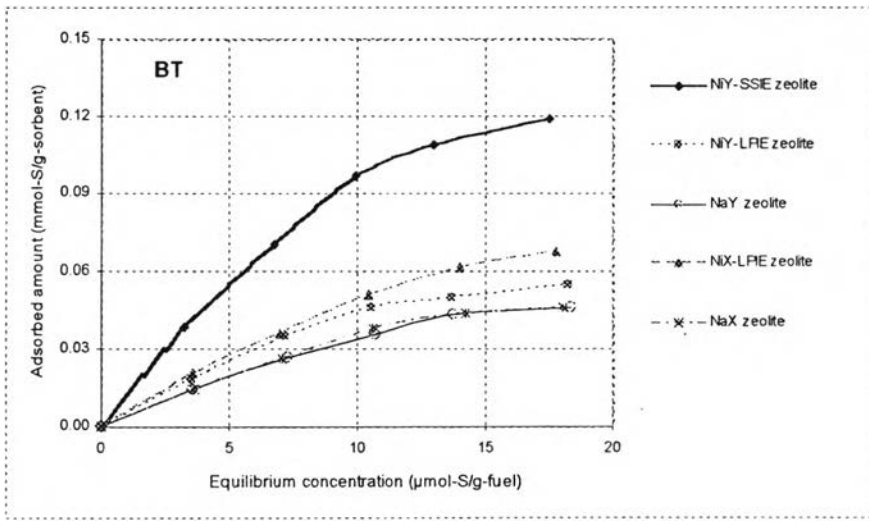

(b)

Figure 4.16 Adsorption isotherms of (a) 3-MT, and (b) BT in benzene solution by various zeolite adsorbents.

Table 4.11 Langmuir parameters of the adsorption of 3-MT and BT in isooctane solution by various zeolite adsorbents

Sulfur compounds	Adsorbent	Q_{max} (mmol-S/g-sorbent)	b (g-fuel/μmol-S)	K_H (g-fuel/g-sorbent)
3-MT	NiY-SSIE (9.17%wt Ni)	2.4734	0.0590	145.9
	NiX-LPIE (7.48%wt Ni)	1.7768	0.0416	73.9
	NiY-LPIE (6.43%wt Ni)	1.2416	0.0505	62.7
	NaX	1.6998	0.0468	79.6
	NaY	1.1905	0.0589	70.1
BT	NiY-SSIE (9.17%wt Ni)	1.2789	0.7786	995.8
	NiX-LPIE (7.48%wt Ni)	1.0746	0.6044	649.5
	NiY-LPIE (6.43%wt Ni)	1.0297	0.5010	515.9
	NaX	0.9088	0.9334	848.3
	NaY	0.8532	0.6808	580.9

Table 4.12 Langmuir parameters of the adsorption of 3-MT and BT in benzene solution by various zeolite adsorbents

Sulfur compounds	Adsorbent	Q_{max} (mmol-S/g-sorbent)	b (g-fuel/μmol-S)	K_H (g-fuel/g-sorbent)
3-MT	NiY-SSIE (9.17%wt Ni)	0.2547	0.0265	6.51
	NiX-LPIE (7.48%wt Ni)	0.1936	0.0240	4.65
	NiY-LPIE (6.43%wt Ni)	0.1724	0.0322	5.55
	NaX	0.1498	0.0304	4.55
	NaY	0.1408	0.0344	4.84
BT	NiY-SSIE (9.17%wt Ni)	0.2912	0.0458	13.34
	NiX-LPIE (7.48%wt Ni)	0.1837	0.0351	6.45
	NiY-LPIE (6.43%wt Ni)	0.1349	0.0446	6.02
	NaX	0.1407	0.0316	4.45
	NaY	0.1307	0.0340	4.44

When comparing all adsorbents, the sorbent capacities for 3-MT and BT removal decreased as follows: NiY-SSIE (9.17%wt Ni) > NiX-LPIE (7.48%wt Ni) > NiY-LPIE (6.43%wt Ni), NaX > NaY for both types of model fuels. The increased capacity, compared with the value obtained by LPIE, confirmed that the SSIE technique was an effective process for the preparation of zeolites. This method proved that not only more metal ions can be incorporated into the framework but also these ions preferably located in exposed active sites, which were impeded in the case of LPIE technique.

When isooctane was used as model fuel, the maximum adsorption capacity of 3-MT on NiY-SSIE zeolite increased by 39% and 99% when compared to that on NiX-LPIE and NiY-LPIE, respectively. In addition, these corresponding, yet lower, values in the case of BT, which were 19% and 24%, indicated that SSIE adsorbent exhibited more adsorption selectivity towards 3-MT than BT.

In contrast to the adsorption in isooctane, the adsorption in benzene showed that SSIE adsorbent was more suitable to remove BT than 3-MT. As the results illustrated, the maximum adsorption capacity of 3-MT on NiY-SSIE zeolite increased by 32% and 48%, in line with 58% and 115% improvement in the case of BT, as compared to that on NiX-LPIE and NiY-LPIE, respectively.

4.3 Dynamic Adsorption of Sulfur Compounds in Simulated Fuels

Our static adsorption studies are expected to illustrate π-complexation type interaction between the exchanged zeolites and sulfur compounds. Therefore, the performance of these ion-exchanged zeolites, serving as interested adsorbents, was subsequently evaluated in the dynamic breakthrough adsorption experiments.

4.3.1 Breakthrough adsorption on Y-type and X-type zeolites

The metal ion-exchanged zeolites were synthesized by loading Ni^{2+} and Cu^{+} on NaX and NaY zeolites under batch exchange and column exchange, respectively,

at ambient conditions. In all cases, 700g of model fuels of isooctane, ~ 400 ppmw sulfur content and 1% by weight of toluene with the flow rate of 5 ml/min were used. The dead volume of the lines before and after the fixed bed reactor was also determined in order to evaluate the cumulative effluent volume. Moreover, to take into account and minimize the effect of water in the model fuels to the breakthrough experiments, the Dependence of the Solubility of Water on Hydrocarbon equation (Constantine Tsonopoulos, 2001) was applied:

$$\ln x_w = \frac{-79.6677 - 6.6547CN}{9.5470 + CN}$$

Where x_w: The solubility of water in hydrocarbon at 298K

CN: Carbon number

Hence, with 700g of the model fuels in our experiments, the maximum concentration of water that is soluble in the feed is 82.4 ppmw (see in Appendices A4.3), much less than 1%wt. This concentration allows the feed to contact with the adsorbent without dehydration pretreatment.

In order to evaluate the strength of the interaction between sulfur compound adsorbate (and toluene) and adsorbent (zeolite), the ratio q/C was calculated, which reflects the relation between the amount of sulfur adsorbed (q) and the concentration of sulfur in the liquid phase (C). As our experiments were performed in low concentration range of sulfur compounds where Henry's law can be applied, the ratio q/C should be approximately equal to Henry's constant (K_H). In addition, a relative selectivity factor for sulfur compounds and toluene, quantitatively demonstrating how sulfur compounds are favored over toluene in a tertiary solution, was used in this study, which is defined as:

$$\alpha_{Sul/Tol} = \frac{q_{Sul}/C_{Sul}}{q_{Tol}/C_{Tol}}$$

Breakthrough adsorption curves of 3-MT and toluene over five different adsorbents are presented in Figure 4.17 (for NaY zeolite), Figure 4.18 (for NiY zeolite), Figure 4.19 (for $Cu^{(I)}Y$ zeolite), Figure 4.20 (for NaX zeolite), and Figure 4.21 (for NiX zeolite), whilst Table 4.13 sumps up the main outcomes.

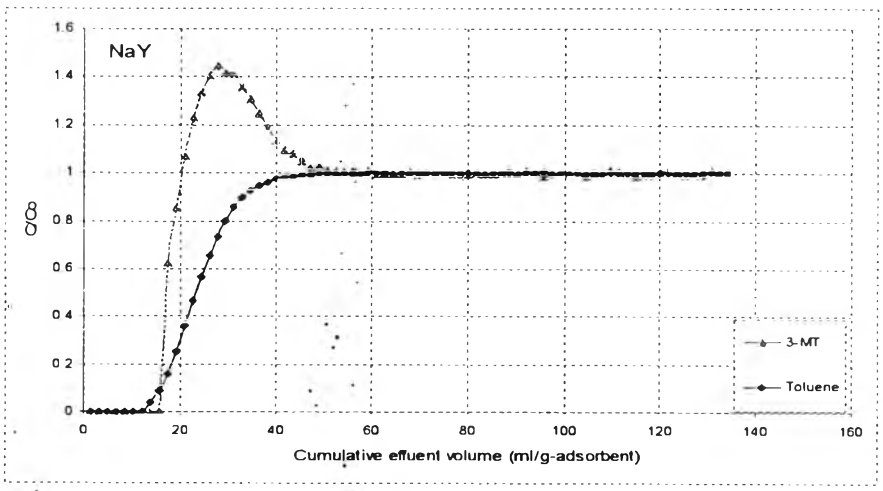

Figure 4.17 Breakthrough curve for the adsorptive removal of 3-MT and Toluene on NaY.

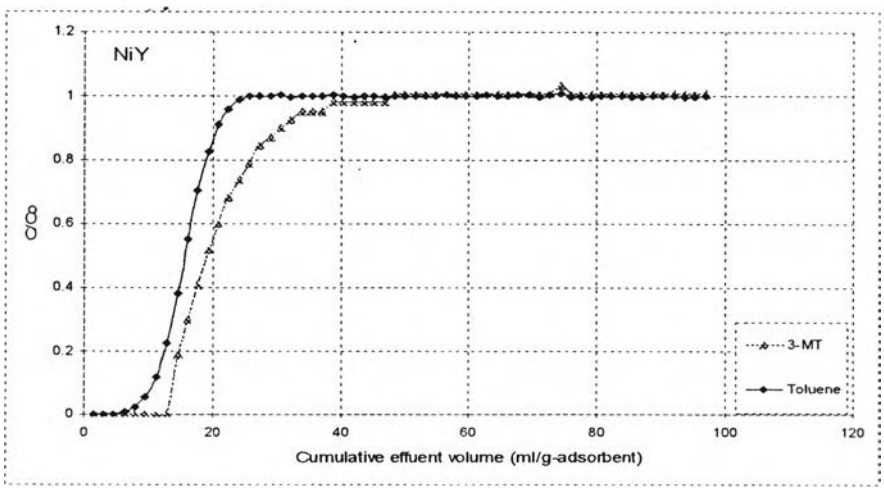

Figure 4.18 Breakthrough curve for the adsorptive removal of 3-MT and Toluene on NiY.

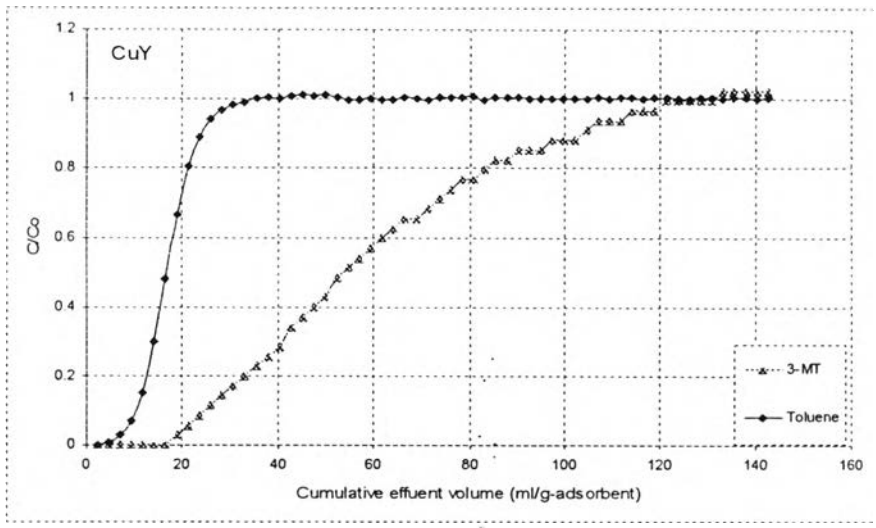

Figure 4.19 Breakthrough curve for the adsorptive removal of 3-MT and Toluene on $Cu^{(I)}Y$.

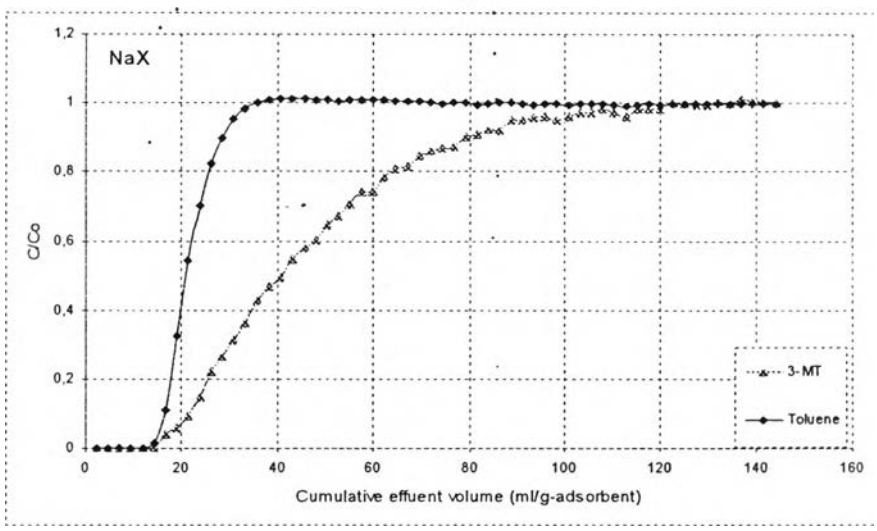

Figure 4.20 Breakthrough curve for the adsorptive removal of 3-MT and Toluene on NaX.

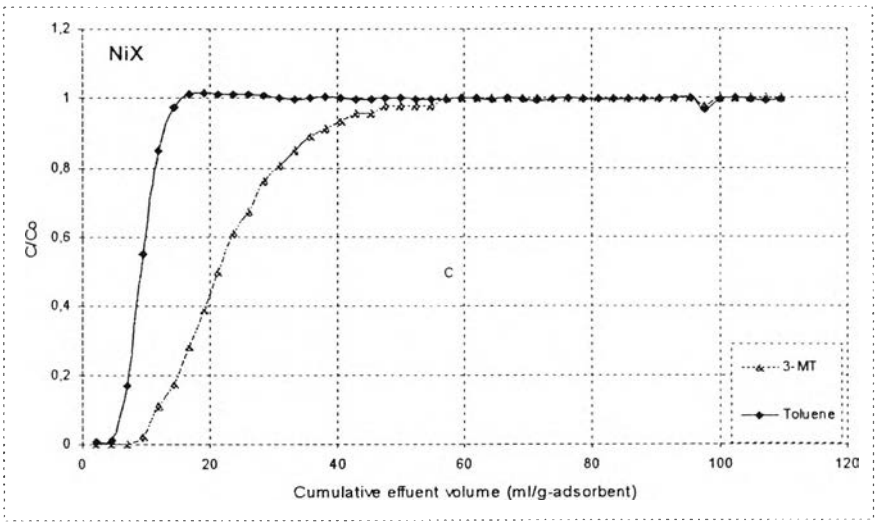

Figure 4.21 Breakthrough curve for the adsorptive removal of 3-MT and Toluene on NiX.

Table 4.13 The equilibrium capacity of different adsorbents for 3-MT and toluene

Zeolite	Sorbate	Cumulative effluent volume (ml/g-zeolite)	Sorbate adsorbed (mg/g-zeolite)	Sorbate Adsorbed (mmol/g-zeolite)	Henry's constant K_H	Selectivity $\alpha_{3mt/Tol}$
NaY	3-MT	10.8	0.7	0.007	2.6	0.4
	Toluene	24.4	45.1	0.49	6	
NiY	3-MT	22.5	1.6	0.02	6.3	1.3
	Toluene	17.1	36	0.39	4.8	
$Cu^{(I)}Y$	3-MT	60.6	4.9	0.05	20.2	3.5
	Toluene	17.1	30.1	0.33	3.9	
NaX	3-MT	46.6	3.3	0.03	13.1	2.1
	Toluene	22.1	30.5	0.33	4	
NiX	3-MT	23.4	2.1	0.02	6.6	2.5
	Toluene	9.5	20.9	0.23	6.7	

As given in Table 4.13, one gram of Cu(I)Y zeolite was capable of removing 4.9 mg 3-MT/g-zeolite. This equilibrium capacity was about 3 times higher than that of NiY zeolite (1.6 mg 3-MT/g-zeolite) and 7 times higher than that of original NaY zeolite (0.7 mg 3-MT/g-zeolite). The findings conclusively indicated that Cu^{+} possesses stronger affinity with 3-MT via π-complexation bonds than Ni^{2+}. This is a clear evidence of a successful autoreduction of Cu^{2+} species to Cu^{+} after 12 hours in helium at 450°C, which is a prerequisite for π-complexation bond forming. It is also suggested that the sulfur adsorptive capacity observed with $Cu^{(I)}Y$ zeolite in our experiments may be further enhanced by improving the conversion of Cu^{2+} to Cu^{+} in the activation process, which was not investigated within this study's scope. Takahashi *et al.* found that 50% of Cu^{2+} was reduced to Cu^{+} after 1h treatment in helium at 450°C; whereas Gedeon *et al.* found that a treatment in helium under similar conditions for 12h yields 75% autoreduction.

Furthermore, NiY zeolite and $Cu^{(I)}Y$ zeolite showed the same trends regarding adsorptive selectivity ($\alpha_{Sul/Tol}$ = 1.3 v.s 3.5). It means that these adsorbent exhibit higher affinity for sulfur compounds in comparison to aromatics. On the other hand, the original NaY zeolite illustrated a less-than-one value of selectivity for 3-MT over toluene (0.4), effectively shifting the affinity scale to toluene. One interesting phenomenon obtained from the removal 3-MT over NaY zeolite is that the C/C_o value of 3-MT escalated over 1.4. After that, it sharply decreased to 1, followed by an increase of toluene C/C_o up to 1 (the point that the adsorbent was totally in equilibrium with toluene). This can be explained that both 3-MT and toluene concurrently adsorbed onto NaY zeolite until the adsorbent reached equilibrium. Afterwards, 3MT molecules, possessing lower adsorptive affinity, tend to be replaced by toluene molecules with stronger adsorptive affinity. Thus, the adsorption of 3-MT on NaY zeolite is reversible: adsorption/desorption. As seen in Figure 1, the below area between the line C/C_o=1 and the breakthrough curve represents the amount of sulfur adsorbed, while the upper area between the line C/Co = 1 and the breakthrough curve represents the amount of 3-MT replaced. In addition, the area between the two breakthrough curves of adsorbates

provides further information about the competitive adsorption of different species on the adsorbents.

In our studies, we conducted the preparation of $Cu^{(I)}X$ zeolite using reduction step under He at high temperature (450°C), the same procedure to obtain $Cu^{(I)}Y$ zeolite. But, the results observed from both N_2 adsorption and breakthrough curve apparently indicated that the structure of $Cu^{(I)}X$ zeolite was destroyed during the activation process. The reason for this undesirable phenomenon is because of low hydrothermal stabilities of X-zeolite, which had been discussed previously in this report. As seen in Figure 4.20 and Figure 4.21 the cumulative effluent volume corresponding to the first moment of breakthrough curve was 46.6 and 23.4 ml/g-zeolite, for NaX and NiX zeolites, respectively, resultant the equilibrium capacities of 3.3 and 2.1 mg 3MT/g-zeolite. In contrast to the adsorption on Y-type zeolite, the metal ion-exchanged X-type zeolite showed lower adsorption capacity than the original one. It is caused by the appearance of mesopore in structure of NiX zeolite, which is demonstrated in Nitrogen adsorption/desorption at 77 K (Figure 4.22).

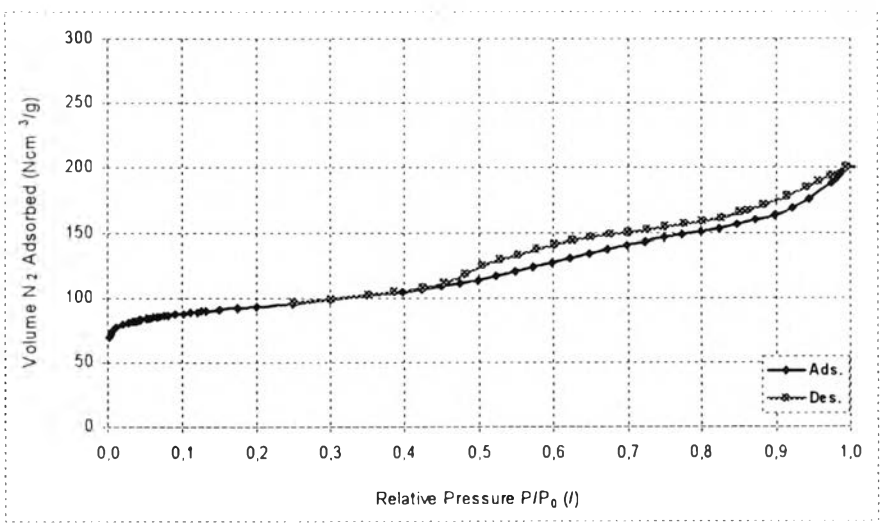

Figure 4.22 Nitrogen adsorption/desorption at 77 K of NiX .

Although the adsorption capacity of NiX is not high as compared with NaX, the selectivity factor also presented a high affinity towards 3-MT (2.5 for NiX zeolite compared with 2.1 for NaX zeolite). Again, this conclusively indicates that π-complexation bond forming between aromatic and adsorbent is not as strongly as the sulfur compounds.

In summary, the equilibrium capacity for 3-MT adsorption increased in the order of NaY < NiY < NiX < NaX < $Cu^{(I)}Y$; while the relative selectivity factor for 3-MT over toluene exhibited the trend NaY < NiY < NaX < NiX < $Cu^{(I)}Y$; under dynamic conditions. Consequently, in both selectivity and capacity, $Cu^{(I)}Y$ zeolite is the best adsorbent.

4.3.2 Effect of pre-adsorbed water on zeolite on sulfur compounds adsorption

It is a well-known fact that zeolite would loose its sulfur adsorption capacity in the presence of compounds which have high affinity with adsorbent. One typical example of these competitors is moisture, present in transportation fuels, which is adsorbed substantially on zeolites. In addition, an interesting effect observed for pre-adsorbed water was that it could be alter the adsorption selectivity between sulfur and aromatics by modifying the interaction between sulfur molecules and metal cations on zeolite. Therefore, it is very important to understand the effect of moisture on the overall adsorption performance.

Due to water's intrinsically poor solubility in hydrocarbon, it was very difficult to dissolve water in the model fuel. For this reason, our experiments were carried out using adsorbent with pre-adsorbed water. The water content chosen here equaled to 4 wt % and 5.7 wt % per gram of NaY and NaX zeolites, respectively, corresponding to approximately one water molecule for two cationic sites on adsorbent. As compared with the maximum water content which is maybe saturated in the feed (82.4 ppmw), the pre-adsorbed concentration is to a great extent higher. Thus, the effect of water from the feed adsorbing on zeolite or pre-adsorbed water on zeolite desorbing to the feed could be neglected. Also in these experiments, the feeds were allowed to

contact with the pre-occupied adsorbent without dehydration pretreatment. The breakthrough capacities of different adsorbents with pre-adsorbed water for 3-MT and Toluene are given in Table 4.14.

Table 4.14 The equilibrium capacity of different adsorbents with pre-adsorbed water for 3-MT and Toluene

Zeolite	Sorbate	Cumulative effluent volume (ml/g-zeolite)	Sorbate adsorbed (mg/g-zeolite)	Sorbate Adsorbed (mmol/g-zeolite)	Henry's constant K_H	Selectivity $\alpha_{Sul/Tol}$
NaY+H_2O	3-MT	7.84	0.41	0.0042	1.13	0.4
	Toluene	17.71	20.22	0.22	2.55	
NiY+H_2O	3-MT	15.7	1.59	0.016	4.43	1.13
	Toluene	13.8	28.21	0.31	3.9	
$Cu^{(I)}Y$+H_2O	3-MT	37.74	3.1	0.031	10.9	3.3
	Toluene	11.82	25.17	0.27	3.3	
NaX+H_2O	3-MT	20.7	1.62	0.016	6.9	1.6
	Toluene	13.1	32.51	0.35	4.4	
NiX+H_2O	3-MT	7.96	0.61	0.006	2.65	1.3
	Toluene	6.17	15.81	0.17	2.06	

It can be seen that in the presence of pre-adsorbed water, the equilibrium capacity for sulfur removal process decreased in comparison to that without water (Figure 4.23, for NaX zeolite). With respect to Y-type zeolites, the equilibrium capacity dropped to about 0.2 mg 3-MT/g-zeolite for NaY and 1.8 mg 3-MT/g-zeolite for $Cu^{(I)}Y$, whereas the change was not apparent in case of NiY. This corresponds to decreases of 13% and 5.7 % on the selectivity for NaY and $Cu^{(I)}Y$ zeolites, respectively. As for X-type zeolites, the influence of pre-adsorbed water seemed to be more significant. It is observed that there was a considerable decrease in terms of equilibrium capacity to 1.68 mg 3-MT/g-zeolite for NaX and 1.5 mg 3-MT/g-zeolite for NiX, which led to a

selectivity reduction of about 24% and 48%. These results indicated that the presence of pre-adsorbed water on adsorbent is detrimental to the π-complexation bonding between adsorbent and sulfur compounds. This is attributed to the stronger bonding strength of water with the adsorbent than that of sulfur compounds. Previously, Yingwei Li *et al.* (2006) had also reported similar results with respect to the relative strengths of bonding: water > thiophene, as predicted from molecular orbital calculation. Therefore, the moisture pre-treatment in order to achieve high sulfur capacity has proven to be imperative target for industrial desulfurization applications which are aiming at sulfur content at ppm level.

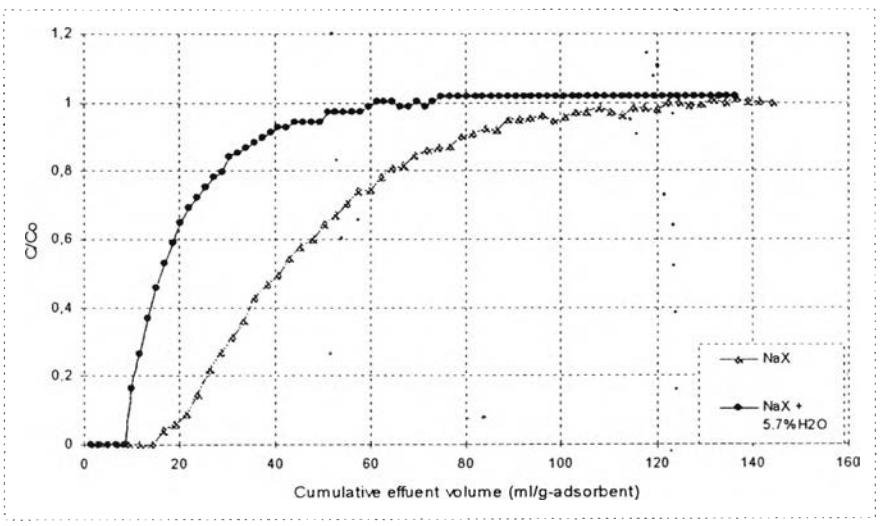

Figure 4.23 Breakthrough curve for the adsorptive removal of 3-MT on NaX zeolite and NaX zeolite with pre-adsorbed water.

Hernandez *et al.* (2004) reported that the cation sites in Y-type zeolite prefer to expose to sites S_{II} where the nucleophilic (aromatic ring, S atom) of adsorbate molecules can interact with. For the case of X-type zeolite, when increasing Si/Al ratio the cationic ions preferably occupy sites S_{III} where the cationic charges are located inside the α-cage. Thus, the cation position in X-zeolites contributes to the higher sulfur compounds adsorption due to the closer interaction between the nucleophilic part and

the cationic charge. Yet, with the presence of water on zeolite, these pre-adsorbed molecules seemed to impede the adsorption energy of sulfur compounds with X-type adsorbents. This consequently results in a significant decrease of adsorption capacity as compared with Y-type zeolites.

Finally, another problem associated with moisture is the stability of $Cu^{(I)}Y$ zeolite, the best adsorbent investigated in this study. As previously reported (Hernandez *et al.*, 2004), Cu^{+} ions are highly unstable, particularly in the presence of moisture. The auto-reduced mechanism for copper exchanged Y-zeolite is known as follows:

$2\ Cu^{+} \leftrightarrow Cu^{2+} + Cu^{0}$, which makes copper ions can not form π-complexation bonding with sulfur molecules.